

# The Cation–Dinitrogen Interaction in the “Benzylidiazonium Ion”: Preferential Electrostatic Complex Formation and Dinitrogen Catalysis of Benzyl Cation Rotational Automerization\*\*

Rainer Glaser\* and David Farmer

Dedicated to Professor Günter Häfeli on the occasion of his 60th birthday

**Abstract:** Diazonium ions are reactive intermediates in deamination reactions pertinent to chemical carcinogenesis. While methylidiazonium ion has been shown to exist as a short-lived intermediate in the gas phase and in solution, benzyldiazonium ions have never been observed, and the reaction intermediates in deaminations of benzyl systems remain a matter of debate. We therefore studied the benzyl cation–dinitrogen interaction by ab initio methods; several important conclusions resulted. Analysis of the potential energy surface at the level MP4(sdtq)/6-31 G\*//MP2(full)/6-31 G\* +  $\Delta$ VZPE(MP2(full)/6-31 G\*) revealed that a classical “benzyldiazonium ion” does not exist. The interaction of N<sub>2</sub> with benzyl cation **M-1** results in an electrostatically bound com-

plex **2C** with a long C–N distance (2.935 Å) as the most stable structure. A covalently bound planar benzyldiazonium ion **2A** with a “normal” C–N bond length (1.514 Å) is the transition-state structure for automerization of the electrostatic complex with concomitant rotation about the exocyclic C–C bond. The potential energy surface characteristics result from the highly efficient  $\pi$ -dative Ph  $\rightarrow$  CH<sub>2</sub> bonding in **M-1**; this is clearly demonstrated in its structure and that of its transition state for rotational automer-

ization **TS-1** by the very high activation barrier for rotation (47.6 kcal mol<sup>-1</sup>) and by the gradient vector fields of the total electron densities of conformers of **1** and **2**. The rotational barrier for **1** is reduced to 27.9 kcal mol<sup>-1</sup> in the N<sub>2</sub> complex **2**, and the potential energy surface characteristics of benzyldiazonium ion essentially facilitate the N<sub>2</sub>-catalyzed rotational isomerization of benzyl cation. The benzyldiazonium ion system shows for the first time that the interaction of a donor molecule with a carbenium ion with a valence LUMO can lead to the formation of an electrostatic complex as opposed to dative bond formation. Dative  $\sigma$ -bond formation between N<sub>2</sub> and the CH<sub>2</sub> carbon of **1** is energetically not competitive with dative Ph  $\rightarrow$  CH<sub>2</sub>  $\pi$ -bond formation.

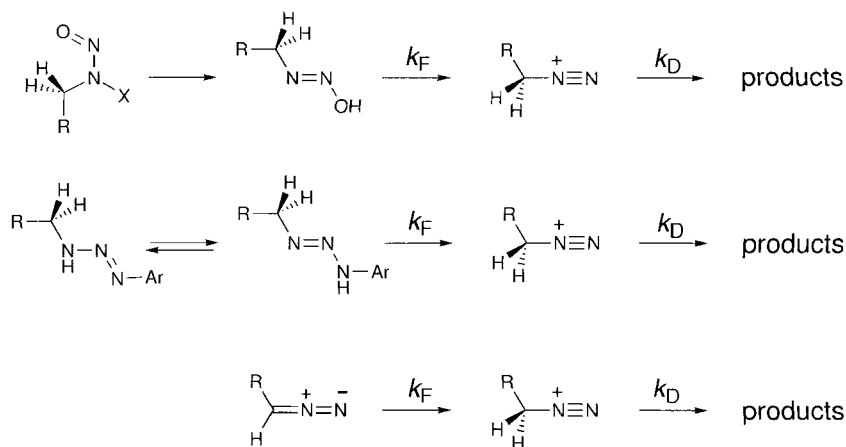
## Keywords

ab initio calculations · benzyldiazonium ion · dative bonding · electrostatic interactions · gas-phase chemistry

## Introduction

Diazonium ions<sup>[1]</sup> are thought to play a crucial role in chemical carcinogenesis.<sup>[2]</sup> A variety of amine derivatives form alkylidiazohydroxides, which can be heterolysed to diazonium ions as the primary alkylating reagents (Scheme 1).<sup>[3–4]</sup> The determination of accurate binding energies and the characterization of diazonium ions are therefore pertinent to discussions of mechanisms of chemical carcinogenesis, and we have studied the formation of dative bonds be-

tween N<sub>2</sub> and carbenium ions.<sup>[5]</sup> The approach of N<sub>2</sub> to a cation with a valence electron sextet leads to internal polarization of N<sub>2</sub>, and the binding energy steadily increases as the initial electrostatic attraction progresses to dative bond formation.<sup>[6]</sup> The-



Scheme 1. Decomposition paths that may involve benzyldiazonium ion (R = Ph).

[\*] Prof. Dr. R. Glaser, D. Farmer  
Department of Chemistry, University of Missouri–Columbia  
Columbia, Missouri 65211 (USA)  
Fax: Int. code + (573) 882-2754  
e-mail: chemrg@showmc.missouri.edu

[\*\*] Presented in part in the *Computers in Chemistry* Division at the 212th National ACS Meeting, Orlando (FL), August 1996, and in the *Physical Chemistry* Division at the 31st Midwest Regional Meeting of the American Chemical Society, Sioux Falls (South Dakota), November 1996.

oretical<sup>[7, 8]</sup> and experimental<sup>[7, 9, 10]</sup> studies have established that this bonding pattern applies generally to many carbon-centered cations. The decompositions of benzyl systems ( $R = Ph$  in Scheme 1) may follow the same mechanisms but the nature of the intermediates remains controversial. While methyl-diazonium ion has been unequivocally shown to exist as a reactive intermediate in the gas phase<sup>[11]</sup> and in aqueous solution,<sup>[12]</sup> benzyldiazonium ions have never been observed directly.<sup>[13]</sup> Studies of the putative benzyldiazonium ion in solution have focused on protonation reactions of aryldiazomethanes and on heterolyses of diazoates and triazenes (Scheme 1). Early solution studies were concerned with the protonation of diazomethanes.<sup>[14–16]</sup> Benzyldiazonium ions had been postulated as stable species in proton-transfer reactions of phenyldiazomethanes but labeling experiments contradicted this hypothesis.<sup>[14]</sup> The early physical–organic studies of the acid-catalyzed decompositions of phenyldiazomethanes by Jungelt and Berseck<sup>[15]</sup> and by Dahn and Diderich<sup>[16]</sup> established the proto-

nation as the rate-limiting step. Finneman and Fishbein<sup>[17]</sup> studied the pH dependence of the protonation of aryldiazomethanes. Biphase behaviour ( $k_o = k_{acid}[H^+] + k_{water}$ ;  $\rho_{acid} = -1.14$  and  $\rho_{water} = -2.01$ ) was found and a common mechanism for both reactions was deduced. These authors also investigated decompositions of (*E*)-arylmethanediazoates in comparison to the aryldiazomethanes.<sup>[18]</sup> The unimolecular decomposition of diazoic acid was found to be the rate-limiting step in the decomposition of the (*E*)-arylmethanediazoates. For the 3,5-bis(trifluoromethyl)phenyl compound it was concluded that the decomposition proceeds via a free diazonium ion intermediate.<sup>[18]</sup> While the rate-limiting step for product formation is likely to be common to all of the substrates included in the study, the ratios of products formed are sensitive to substrate characteristics. The azide solvent selectivities measured for the decompositions of (3,5-bis(trifluoromethyl)phenyl)diazomethane and of (3,5-bis(trifluoromethyl)phenyl)diazoate indicate that the same free diazonium ion intermediate is formed in both decompositions. For the unsubstituted pair, on the other hand, the azide solvent selectivities are different. The observed linear Hammett plot for the decompositions of substituted phenylmethanediazoic acids ( $\rho = -1.23$ ) was interpreted as evidence for diazonium ion formation in the rate-limiting step in all cases. The reaction constant is negative and only slightly larger in magnitude than the reaction constant for the protonation of benzylamines ( $\rho = -1.07$ ). We find this result surprising, since one would expect a significant increase in the magnitude of  $\rho$  as there is more positive charge on the hydrocarbon fragment of the diazonium ion compared to the ammonium ion. The absence of this more negative  $\rho$  indicates that the “benzyldiazonium ion” intermediate has hardly formed in the transition state of the rate-limiting step, and that the transition states are early with regard to the N–O cleavage. Triazenes are closely related to diazoic acids, and the same mechanistic issues arise. Sinnott et al.<sup>[19]</sup> studied the dissociations of substituted benzyl-aryl triazenes  $X-Ph-CH_2-N=N-NH-Ar$  ( $X = H, NO_2, Cl, Br, Me, OMe$ ) in aqueous solution. It was claimed that the benzyldiazonium ion was a “free, solvent-equilibrated intermediate” because the physical–organic evidence shows that the N–N bond cleavage is rate-limiting in both the acid-catalyzed and the pH-independent decomposition reactions.

Thus, the physical–organic solution phase studies of the heterolyses of diazoates and triazenes as well as the protonations of the diazomethanes all show that the step leading to the presumed benzyldiazonium ion intermediate is rate-limiting. These results *do not imply the existence* of benzyldiazonium ion but, rather, *allow for the existence* of benzyldiazonium ion and its fast decomposition ( $k_D > k_F$ ) in these processes. On the other hand, the results are entirely compatible with any degree of C–N bond cleavage after the transition state of the rate-limiting step has been traversed. In a recent study of decompositions of benzyl systems, White et al. proposed the so-called Inert-Molecule-Separated Ion Pair hypothesis, which holds that nitrogen-separated ion pairs play a key role in the mechanisms of these reactions in nonpolar solvents.<sup>[20]</sup> The question as to the existence of the benzyldiazonium ion and the nature of the C–N interaction between benzyl cation and dinitrogen remains unanswered to this day. In this article, we report the results of an ab initio study of “benzyldiazonium ion” to address some funda-

**Abstract in German:** *Diazonium-Ionen sind reaktive Zwischenstufen in Desaminierungsreaktionen, die im Hinblick auf die Krebsentstehung von Bedeutung sind. Das Methyl-diazonium-Ion kann als kurzlebige Intermediat in der Gasphase und in Lösung existieren. Im Gegensatz dazu konnten Benzyldiazonium-Ionen noch nicht beobachtet werden, und die Reaktionszwischenstufen in Desaminierungen von Benzylsystemen bleiben umstritten. In diesem Zusammenhang haben wir die Benzylkation-Distickstoff-Wechselwirkung mit ab-initio-Methoden studiert und dabei wichtige Ergebnisse erhalten. Potentialhyperflächenanalyse auf dem Niveau MP4(sdtq)/6-31G\*/MP2(full)/6-31G\* +  $\Delta VZPE(MP2(full)/6-31G^*)$  zeigte, daß das klassische Benzyldiazonium-Ion nicht existiert. Die Wechselwirkung zwischen  $N_2$  und dem Benzylkation **M-1** ergibt einen elektrostatisch gebundenen Komplex **2C** mit einer langen C–N-Bindung (2.935 Å) als stabilste Struktur. Das kovalent gebundene, planare Benzyldiazonium-Ion **2A** mit “normaler” C–N-Bindungslänge (1.514 Å) ist eine Übergangszustandsstruktur für die Automerisierung des elektrostatischen Komplexes mit gleichzeitiger Rotation um die exocyclische C–C-Bindung. Diese Eigenschaften der Potentialhyperfläche resultieren aus der hochwirksamen  $\pi$ -Donor  $Ph \rightarrow CH_2$ -Bindung im Benzylkation **M-1**. Klare Indizien für diese  $\pi$ -Donorbindung finden sich in der Struktur von **M-1** und in der Struktur **TS-1** des Übergangszustandes für die Rotations-Automerisierung, in der sehr hohen Rotationsbarriere (47.6 kcal mol<sup>-1</sup>) und in den Gradientenvektorfeldern der Gesamtelektronendichten konformerer Strukturen von **1** und **2**. Die Rotationsbarriere von **1** wird im  $N_2$ -Komplex **2** auf 27.9 kcal mol<sup>-1</sup> reduziert, und die Potentialfläche des “Benzyldiazonium-Ions” kann beschrieben werden als die Potentialhyperfläche eines  $N_2$ -Komplexes, der die “ $N_2$ -katalysierte Rotations-Isomerisierung des Benzylkations” sehr erleichtert. Das Benzyldiazonium-Ion zeigt zum ersten Mal, daß die Wechselwirkung zwischen einem Donormolekül und einem Carbenium-Ion mit einem Valenz-LUMO zur bevorzugten Bildung eines elektrostatischen Komplexes führen kann. Die dative  $\sigma$ -Bindungsbildung zwischen  $N_2$  und dem  $CH_2$ -Kohlenstoffatom in **1** ist nicht wettbewerbsfähig mit der dativen  $Ph \rightarrow CH_2$ - $\pi$ -Bindungsbildung.*

mental issues regarding the cation–dinitrogen interaction in the “benzyl diazonium ion”. We will show that the interaction of  $N_2$  with benzyl cation **1** results in an electrostatically bound complex **2C** with a long C–N distance as the most stable structure. A covalently bound benzyl diazonium ion **2A** serves as the transition-state structure for automerization of the electrostatic complex with concomitant rotation about the exocyclic bond. The “benzyl diazonium ion” system represents the first case in which the interaction of a donor molecule with a cation with a valence LUMO does not lead to dative bonding but remains limited to electrostatic interactions alone. The origin of the unexpected potential energy surface characteristics lies with the highly efficient  $\pi$ -dative  $Ph \rightarrow CH_2$  bonding in the benzyl cation. The implications with regard to the involvement of benzyl diazonium ions in deamination reactions are discussed and strategies are described that may guide the search for other electrostatic complexes of this type.

### Computational Methods

Potential energy surfaces were examined with restricted Hartree–Fock (RHF) theory and with the inclusion of electron correlation at the second-order level of Møller–Plesset theory (MP2) with all electrons included in the active space.<sup>[21, 22]</sup> Energies were also determined at the full fourth-order level of Møller–Plesset perturbation theory, MP4(sdtq),<sup>[23]</sup> for the MP2 optimized structures and with all electrons included in the active space. This high level of perturbation theory provides an accuracy that comes close to quadratic configuration interaction (QCI) and coupled cluster (CC) methods.<sup>[24]</sup> We showed previously for various diazonium ions  $RN_2^+$  ( $R = H$ ,<sup>[7a]</sup> Me,<sup>[5a, b]</sup> Et,<sup>[5a]</sup> Ph<sup>[8]</sup>) that this theoretical level is more than adequate. The 6-31 G\* basis set was used throughout and six Cartesian d-type basis functions were employed. All structures were optimized in  $C_{2v}$  and  $C_s$  symmetry, respectively, by gradient techniques; constraints were applied to the CN bond lengths to determine cross-sections of the potential energy surface. The first and second energy derivatives were computed analytically at RHF/6-31 G\* and MP2(full)/6-31 G\* levels to confirm that stationary structures were indeed obtained and to determine harmonic vibrational frequencies. Vibrational zero-point energy corrections to binding energies and activation barriers were scaled by factors 0.9135 (RHF/6-31 G\*) and 0.9646 (MP2/6-31 G\*).<sup>[25]</sup> The results of the computations are summarized in Table 1.

Calculations were performed with the program Gaussian94<sup>[26]</sup> on IBM RS-6000 systems on the MU Cluster and the SP2 of the Cornell Theory Center. The MP4 calculations were performed on an SGI PowerChallenge L system. Molecular orbital plots were generated with the program Spartan<sup>[27]</sup> on a Power Macintosh 9500/120. The color-coded gradient vector fields of the electron density distributions were computed with the program CCGVF,<sup>[28]</sup> which combines the display of the gradient vector field lines and of the molecular graph<sup>[29]</sup> with information about the magnitude of the electron density through color coding. The CCGVF plots were generated on a Silicon Graphics Indigo workstation.

### Results and Discussion

**Benzyl cation:** Theoretical studies of the benzyl cation, **1**, date back to 1976 when Hehre et al.<sup>[30]</sup> provided evidence that **1** can exist in the gas phase, although it is thermodynamically less stable than the tropylium ion.<sup>[31, 32]</sup> Calculations at the HF/6-31 G//HF/3-21G level predicted a preference of 7.6 kcal mol<sup>-1</sup> for the tropylium ion over **1**.<sup>[33]</sup> The rotational barrier of **1** has not been measured to date. Four recent theoretical papers examined the double-bond character of the exocyclic bond. It was established that the planar and  $C_{2v}$ -symmetric minimum structure **M-1** is the most stable structure and that the nonplanar  $C_{2v}$ -symmetric structure **TS-1** is the transition state structure for rotation. Houk et al.<sup>[34]</sup> reported the RHF/3-21G structures of **M-1**<sup>[34b]</sup> and **TS-1**, and discussed the rotational barrier of 45.4 kcal mol<sup>-1</sup>, the short  $C_{ipso}$ – $CH_2$  bond length of 1.356 Å in **M-1**, and the resonance stabilization energy of 38.6 kcal mol<sup>-1</sup> as indicators of strong  $\pi$  donation from the phenyl ring into the  $CH_2$  p AO of the planar **M-1**. Mulliken population analyses of **M-1** at the RHF/STO-3G and RHF/4-31G levels by Ohwada and Shudo indicate ring charges in excess of +0.6 and a high double-bond character of the exocyclic  $C_{ipso}$ – $CH_2$  bond.<sup>[35]</sup> These results were greatly expanded upon by the study of Nakata et al. in which the resonance demand factors  $r$  of the Yukawa–Tsunoo equation were compared to resonance indices (bond lengths, Mulliken populations, and bond orders) of the RHF/6-31 G\* structures of 14 benzyl cations  $[Ph-CR, R_2]^+$ .<sup>[36]</sup> Eiden et al. recently reported the equilibrium structure and a detailed vibrational analysis of **M-1** at the MP2(full)/6-31 G\* level, in which very good agreement between experiment and theory was obtained.<sup>[37]</sup> The only available theoretical study of the rotational barrier did not employ polarized basis sets and the consideration of electron correlation effects as well was prohibited at the time by the size of the system.<sup>[38]</sup> In light of the rather high barriers to rotation (>45 kcal mol<sup>-1</sup>) predicted at the RHF levels, it seemed pertinent to examine the rotational barrier of the benzyl cation with a larger, polarized basis set and with the inclusion of electron correlation. We have optimized **M-1** and **TS-1** at the MP2(full)/6-31 G\* level; the optimized structures are shown in Figure 1. The rotational barrier is 45.9 kcal mol<sup>-1</sup> at the RHF/6-31 G\* level and 49.1 kcal mol<sup>-1</sup> at the MP2(full)/6-31 G\* level. The vibrational zero-point energy of **M-1** exceeds that of **TS-1** by 1.8 and 2.2 kcal mol<sup>-1</sup>, respectively, at the RHF/6-31 G\* and MP2(full)/6-31 G\* levels, and this difference reduces the rotational barrier by about

Table 1. Total and vibrational zero-point energies (total energies in atomic units and unscaled vibrational zero-point energies (VZPE) in kcal mol<sup>-1</sup>) [a].

Molecule	RHF				MP2				MP <sub>x</sub> /MP2		
	C–N	E(RHF)	VZPE	N [b]	C–N	E(MP2)	VZPE	S [c]	N [b]	E(MP3)	E(MP4(sdtq))
<b>1</b> , Ph–CH <sub>2</sub> <sup>+</sup>											
<b>M-1</b> , $C_{2v}$	1.3574	–268.886732	78.87	0	1.3721	–269.776757	74.12	74.31	0	–269.812280	–269.867036
<b>TS-1</b> , $C_{2v}$	1.4544	–268.813607	76.87	1	1.4214	–269.698585	71.89	78.83	1	–269.733657	–269.787586
$N_2$		–108.943950	3.94	0		–109.261574	3.12	45.87	0	–109.251950	–109.278925
<b>2</b> , PhCH <sub>2</sub> N <sub>2</sub> <sup>+</sup>											
<b>2A</b> , $C_s$ , in plane	1.5412	–377.771923	85.47	1	1.4666	–379.006461	79.73	83.09	1	–379.023315	–379.108750
<b>2C'</b> , $C_s$ , perp.	1.5412 (f)	–377.782707			1.4666 (f)	–379.015156				–379.031099	–379.116997
<b>2C</b> , $C_s$ , perp.	3.3390	377.832867	83.17	0	2.9349	–379.042724	77.77	102.31	0	–379.067239	–379.150041

[a] All data computed with the 6-31 G\* basis set. [b] N indicates the number of imaginary frequencies of the stationary structure. [c] Entropies S in cal mol<sup>-1</sup> K<sup>-1</sup> for standard conditions.

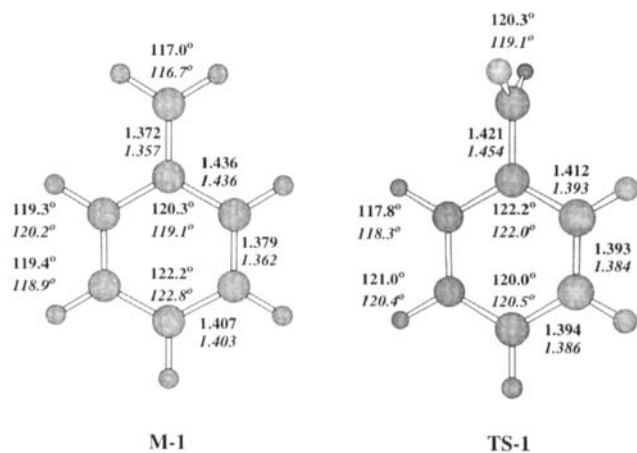


Figure 1. The optimized structures of benzyl cation **M-1** and the transition-state structure for rotational autoionization **TS-1**. Molecular models are shown of the MP2(full)/6-31 G\* optimized structures and structural parameters are given for the MP2(full)/6-31 G\* level and also for the RHF/6-31 G\* level (italics).

2 kcal mol<sup>-1</sup>. Higher levels of perturbation theory affect the rotational barrier only slightly. The activation energies for CH<sub>2</sub> rotation of 49.3 and 49.9 kcal mol<sup>-1</sup> computed at the MP3/6-31 G\*\*/MP2(full)/6-31 G\* and MP4(sdtq)/6-31 G\*\*/MP2(full)/6-31 G\* levels are within 1 kcal mol<sup>-1</sup> of the value determined at the MP2(full)/6-31 G\* level. Our best estimate of the rotational barrier is 47.7 kcal mol<sup>-1</sup> at the level MP4(sdtq)/6-31 G\*\*/MP2(full)/6-31 G\* + ΔVZPE(MP2(full)/6-31 G\*). We conclude that the previously reported high rotational barrier is not an artifact caused by the modest theoretical levels employed. In fact, our higher-level data indicate an even greater rotational barrier that comes close to the rotational barriers of alkenes. Gas-phase measurements of the unimolecular *cis*–*trans* isomerizations on the singlet surfaces of ethene and butene, respectively, gave activation energies of 65 kcal mol<sup>-1</sup> and 51–62 kcal mol<sup>-1</sup>.<sup>[39]</sup>

The CH<sub>2</sub> carbon is trigonal planar in **M-1** and **TS-1**, and the C<sub>ipso</sub>–CH<sub>2</sub> bond is shorter in **M-1** than **TS-1** by 0.049 Å at MP2/6-31 G\*. It is this C<sub>ipso</sub>–CH<sub>2</sub> bond shortening that is the primary structural evidence for stabilization of the primary carbenium ion center by the phenyl substituent by π donation. While the structural changes associated with rotation about the C<sub>ipso</sub>–CH<sub>2</sub> bond show the same trends at the MP2/6-31 G\* and RHF/6-31 G\* levels, RHF theory would predict a much larger C<sub>ipso</sub>–CH<sub>2</sub> bond length difference of 0.097 Å between **M-1** and **TS-1**. A significant structural difference between **M-1** and **TS-1** concerns the magnitude of the bond length alternation in the arene system: these bonds are longer and alternate more in **M-1** (1.407 ± 0.029 Å) than in **TS-1** (1.400 ± 0.012 Å). These structural results are consistent with a larger positive charge in the phenyl ring in **M-1** (less π bonding) and indicate a significant contribution by the quinoid resonance forms to **M-1**. The recent natural resonance theoretical analysis of benzyl systems by Eiden et al. indicates bond orders of 1.7 for the C<sub>ipso</sub>–CH<sub>2</sub> bonds in the benzyl cation and anion, while the corresponding bond order in the radical is only 1.5.<sup>[37a]</sup> These structural results can be readily understood in terms of frontier molecular orbital theory, and pertinent FMOs are displayed in Figure 2. The methylene group perturbs the phenyl π MO that is asymmetric

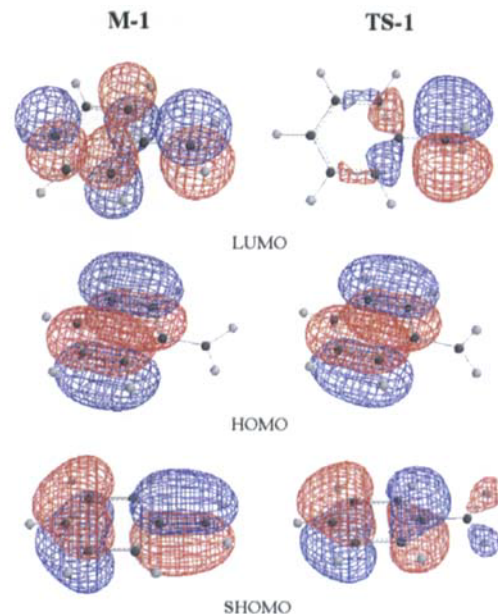
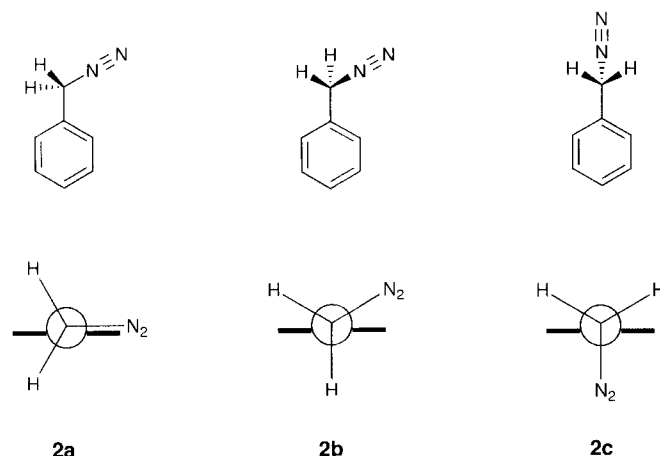


Figure 2. Ab initio computed MOs of benzyl cation **M-1** and of the transition-state structure for rotation about the exocyclic C–C bond **TS-1**. The LUMO in **M-1** is delocalized, while the LUMO in **TS-1** is almost completely localized at the methylene carbon. Strong π-conjugative donation Ph → CH<sub>2</sub> is clearly evident in the SHOMO of **M-1**.

with respect to the main rotational axis (SHOMO). Strong Ph → CH<sub>2</sub> π-conjugative donation is clearly evident in the SHOMO of **M-1**. There are no hyperconjugative interactions across the C<sub>ipso</sub>–CH<sub>2</sub> bond in the SHOMO or LUMO of **TS-1**, and hyperconjugative donation from the C<sub>ipso</sub>–C<sub>ortho</sub> bonds into the in-plane CH<sub>2</sub> p AO plays only a minor role.

Several gas-phase studies provide evidence for the high double-bond character of the exocyclic bond. Tsuno et al. measured chloride ion affinities of substituted benzyl cations using ion cyclotron resonance.<sup>[40]</sup> Linear free energy analysis of the thermochemical data for chloride exchange reactions showed that the resonance demand factor  $r^+ = 1.31$  was higher than that of the 1,1-dimethylbenzyl cation system ( $r^+ = 1.0$ ). These gas-phase results parallel the enhanced resonance effects described with  $\sigma^+$  plots for benzylic solvolyses<sup>[41]</sup> and photosolvolyses.<sup>[42]</sup> Evidence for π stabilization of benzyl cations also stems from Olah's demonstration of the absence of such stabilization mechanisms in highly crowded benzyl cations.<sup>[43]</sup> The relative stabilities computed and measured for 2-, 3-, and 4-chlorobenzyl cations in the gas phase are also consistent with significant contributions by quinoid resonance structures.<sup>[44]</sup> Eiden et al. studied several isotopomers of **1** with zero kinetic energy photoelectron spectroscopy (ZEKE–PES); vibrational frequencies were measured in the range 0–650 cm<sup>-1</sup>.<sup>[37]</sup> The frequencies of the out-of-plane modes were determined indirectly from combination bands and ab initio calculations and provide a quantitative measure of the bond order of the exocyclic C<sub>ipso</sub>–CH<sub>2</sub> bond. It was concluded that **M-1** has a substantially greater double-bond character than the benzyl radical in the CH<sub>2</sub> torsion and quasi-umbrella modes. In particular, Eiden et al. pointed out that the torsional frequency of **M-1** of 627 cm<sup>-1</sup> is similar to those of alkenes.<sup>[37b]</sup>

**Potential energy surface analysis of “benzyl diazonium ion”:** In the course of the RHF/6-31 G\* potential energy surface analysis, several cross-sections were studied; we use small letters to differentiate between these types of structures, while capital letters denote stationary structures. Thus, for example, **2A** is a stationary structure along the cross-section involving structures of type **2a**. We began the potential energy surface analysis of benzyl diazonium ion **2** with that  $C_s$  symmetric conformation in which the diazo function lies in the plane of the benzene ring, **2a** (Scheme 2). Structure **2A** exhibited a C–N bond length of



Scheme 2. Conformations of the benzyl diazonium ion.

1.541 Å (Figure 3) and was found to correspond to a transition-state structure. The displacement vector associated with the imaginary mode of **2A** ( $88 i \text{ cm}^{-1}$ ,  $a''$ ) indicates an out-of-plane bending of the  $-\text{CH}_2\text{N}_2$  function, and we anticipated finding an asymmetrical minimum **2B** in the vicinity of **2A** with a stag-

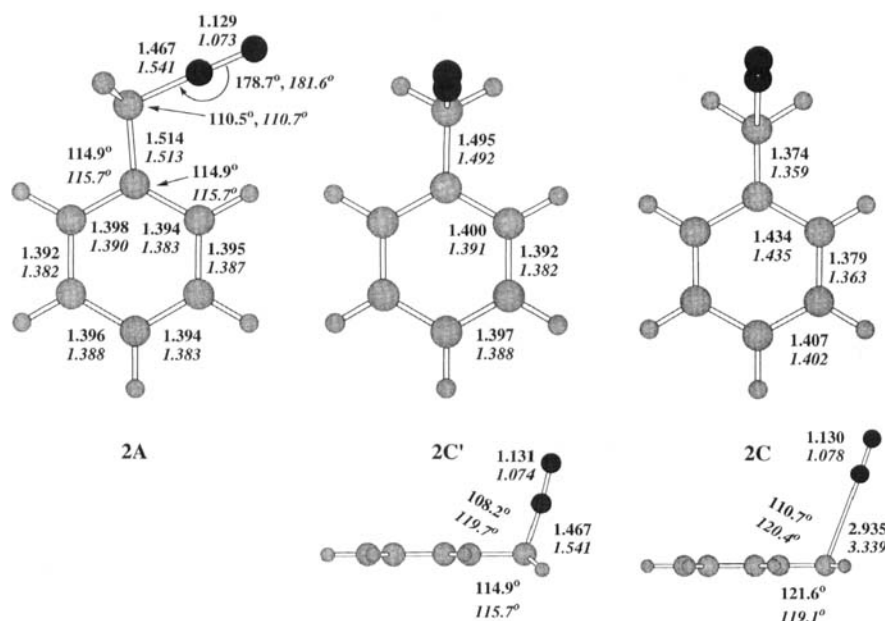


Figure 3. The optimized structures of the electrostatic complex **2C** and of the transition-state structure **2A** of the benzyl diazonium ion. In the model structure **2C** the C–N bond was kept fixed at its value in **2A**. As in Figure 1, molecular models are shown of the MP2(full)/6-31 G\* optimized structures, and structural parameters are given for the MP2(full)/6-31 G\* level and also for the RHF/6-31 G\* level (italics).

gered arrangement about the  $C_{\text{ipso}}-\text{CH}_2$  bond. However, optimization of **2** beginning with a distorted structure **2A** resulted in rotation about the  $C_{\text{ipso}}-\text{CH}_2$  bond such as to realize the staggered arrangement in which the diazo function lies in the  $C_s$  plane perpendicular to the (best) molecular plane of the benzene ring, **2c**, and, surprisingly, the optimization indicated a steadily increasing C–N bond length! We then studied the cross-section with structures of type **2c** (Figure 4). The energy steadily de-

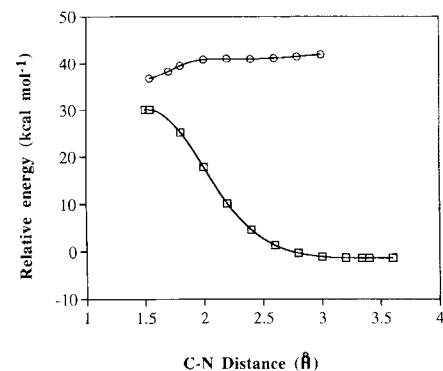


Figure 4. Cross-sections of the potential energy surface of **2** as a function of the C–N bond length for structures of types **2a** (circles) and **2c** (squares). Energies are relative to the combined energies of benzyl cation **M-1** and dinitrogen.

creased as  $d(\text{C}-\text{N})$  increased and a shallow minimum **2C** (Figure 3) was reached at  $d(\text{C}-\text{N}) = 3.339 \text{ \AA}$ . Hence, a “classical” benzyl diazonium ion does not correspond to a minimum on the potential energy surface and such an ion does not exist in the gas phase. The only minimum located on the potential energy surface corresponds to a weakly bound electrostatic complex **2C** between benzyl cation and  $\text{N}_2$ . The potential energy surface characteristics of **2** might seem unexpected and puzzling. For most cations, the approach of  $\text{N}_2$  results in a steady lowering of energy and the formation of a diazonium ion usually without any barrier. In the case of **2**, however, the benzyl cation prefers to form merely an electrostatic complex **2C** as the most stable “diazonium ion” while the diazonium ion structure **2A** with its shorter C–N bond remains higher in energy. At the RHF/6-31 G\* level, the electrostatic complex **2C** is bound by a mere  $1.4 \text{ kcal mol}^{-1}$  and the benzyl diazonium ion type structure **2A** is  $36.9 \text{ kcal mol}^{-1}$  less stable than the isolated fragments benzyl cation +  $\text{N}_2$ . We also optimized a structure **2C** for which we kept the C–N bond length fixed to the value realized in **2A**; this structure **2C'** may serve as a model for the classical staggered benzyl diazonium ion. As can be seen from Table 2, structure **2C'** is slightly favored over **2A** (in part due to reduction of steric interaction with *ortho*-H in **2A**) but is still more than  $30 \text{ kcal mol}^{-1}$  less stable than the free fragments.

Table 2. Rotational barriers and binding energies in kcal mol<sup>-1</sup> [a,b].

Molecule	$\Delta VZPE$ , RHF	$E$ , RHF	$\Delta VZPE$ , MP2	$E$ , MP2	$E$ , MP3	$E$ , MP4
$E_A(1)$	-1.83	45.89	-2.15	49.05	49.34	49.86
$E_b(2A)$ , $C_s$ , in plane	+2.43	36.87	+2.40	20.00	25.67	23.35
$E_b(2C')$ , $C_s$ , perp.		30.10		14.54	20.79	18.18
$E_b(2C)$ , $C_s$ , perp.	+0.33	-1.37	+0.51	-2.76	-1.89	-2.56
$E_A(2)$	+2.10	38.24	+1.89	22.76	27.56	25.91

[a] All energies computed with the 6-31 G\* basis set. The MP3 and MP4(sdtq) energies are based on the MP2(full)/6-31 G\* optimized structures. The  $\Delta VZPE$  values are scaled by factors 0.9135 (RHF) and 0.9646 (MP2). [b] Activation energies  $E_A(1)$  specify the rotational barrier for the benzyl cation. Binding energies  $E_b$  are given for the  $BzN_2^+$  systems with respect to benzyl cation and  $N_2$ . Activation energies  $E_A(2)$  specify the rotational barrier of benzyl cation with  $N_2$  catalysis.

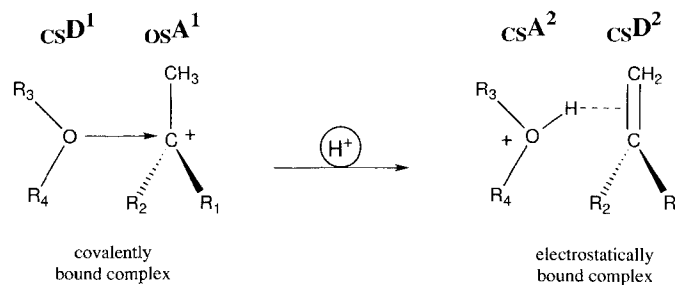
The structures of **2A** and **2C** and of the model **2C'** were refined by optimization at the MP2(full)/6-31 G\* level, and vibrational analyses were carried out for **2A** and **2C** at this level. Furthermore, we computed energies at the full fourth-order level of Møller–Plesset perturbation theory, MP4(sdtq)/6-31 G\*\*//MP2(full)/6-31 G\* for these structures. The results are included in Tables 1 and 2 and they show that *the essential features all persist at these higher levels*. A closer approach of  $N_2$  is indicated in the MP2 structure of **2C**, but the MP2 binding energy of 2.8 kcal mol<sup>-1</sup> again indicates only marginal bonding, and the same is true at the MP4 level. The in-plane transition-state structure **2A** (89.0 i cm<sup>-1</sup>, a'') and the model **2C'** benefit from electron correlation effects and their relative stabilities with regard to the dissociated fragments are significantly reduced.<sup>[45]</sup> As can be seen from Table 1, the vibrational zero-point energies of **2A** and **2C** exceed those of the isolated fragments benzyl cation and  $N_2$  and the vibrational corrections to binding energies  $\Delta VZPE$  are positive (Table 2). Our best estimate for the binding energy of the electrostatic complex **2C** thus becomes 2.1 kcal mol<sup>-1</sup> at the MP4(sdtq)/6-31 G\*\*//MP2(full)/6-31 G\* +  $\Delta VZPE$ (MP2(full)/6-31 G\*) level, while **2A** is 25.8 kcal mol<sup>-1</sup> less stable than the free fragments at that same level. The energy difference between **2C** and **2A** is the activation energy for rotational automerization of **2C** and we find a value of  $E_A(2) = 27.8$  kcal mol<sup>-1</sup> at our best theoretical level. The electrostatic complex **2C** can only exist so long as the binding energy dominates the  $-T\Delta S$  term. The entropy data given in Table 1 result in  $\Delta S = -17.9$  cal mol<sup>-1</sup> K<sup>-1</sup> for the formation of **2C** and suggest that **2C** can exist only below temperatures of about 110 K.

#### Covalently bound and electrostatically bound cation–neutral complexes:

The approach of a neutral polarizable and possibly di- or quadrupolar molecule to a positively charged center will result in dipole induction and alignment; the overall result is an electrostatic attraction that increases as their distance is reduced. The ion–molecule interactions of the lithium<sup>[46a]</sup> and potassium<sup>[46b,c]</sup> cations are good examples. Dative bonding occurs when a covalent component is added to the electrostatic interaction. The primary requirements for dative bonding are the availability of weakly bonded or nonbonded electron pairs on the donor (lone pair or  $\pi$  bond) and a low-lying LUMO on the acceptor. Simple diazonium ions are excellent examples of the latter. While the bonding in the  $N_2$  complexes of the cations  $Li^+$  and  $Na^+$  is primarily electrostatic,<sup>[47]</sup> the interaction of  $N_2$

with the cation  $CH_3^+$  leads to the formation of a dative bond.<sup>[5]</sup> The approach of  $N_2$  to the cation leads to internal polarization of the  $N_2$  group and steadily increases the binding energy; theoretical<sup>[7,8]</sup> and experimental<sup>[7,9,10]</sup> studies have established that the same bonding pattern applies generally to many carbon-centered cations. Significant charge transfer occurs only for more electronegative  $NH_2^+$ ,  $OH^+$ , and  $F^+$  acceptors<sup>[5c,d]</sup> and dative bonding turns into covalent bonding.<sup>[48]</sup> The bonding situation in the cation– $N_2$  systems is thus quite different from Lewis acid–base complexes involving the  $N_2$  donor and neutral Lewis acids. For example, the  $N_2 \cdots BF_3$  complex has long been known as a van der Waals complex with a long B–N bond of 2.875 Å.<sup>[49]</sup>

The formation of electrostatically bound complexes is not limited to complexes involving simple ions with full valence shells (e.g.,  $Li^+$ ); such complexes are also formed with molecular cations that do not have a low-lying valence LUMO. Lias has shown that the bonding in the proton-bound "loose complexes" formed between  $MH^+$  and N ( $M, N = NH_3, PH_3, H_2O, H_2S, HCl$ ) is primarily electrostatic.<sup>[50]</sup> Electrostatically bound complexes often involve unsaturated donors and occur for systems where isomer 1 consists of a complex between a neutral closed-shell donor  $csD^1$  and a cationic acceptor  $osA^1$  with a valence electron sextet. The transfer of a proton or of a cationic fragment<sup>[51]</sup> leads to isomer 2 in which two closed-shell components, namely the cationic acceptor  $csA^2$  and the neutral donor  $csD^2$ , are complexed. Such isomerizations can be described with Brauman's double-well model;<sup>[52]</sup> an example involving the transfer of a proton is illustrated in Scheme 3.

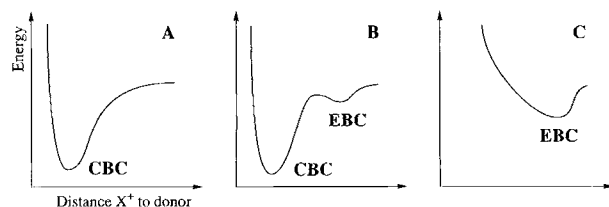


Scheme 3. Electrostatically bound complexes occur with molecular cations that do not have a low-lying acceptor LUMO.

The H-bonded electrostatically bound complexes shown in Scheme 3 were characterized by Norrman and McMahon in their recent study of the generation of complexes between the *tert*-butyl cation and a series of small organic molecules ( $CH_3CN, EtOH, Me_2O, Et_2O, Me_2CO$ ).<sup>[53]</sup> For the systems examined, the low-temperature, covalently bound species were characterized by larger  $-\Delta H^\ddagger$  and  $-\Delta S^\ddagger$  values than the electrostatically bound isomers. Several other experimental observations provide evidence for electrostatic complexes involving closed-shell molecular cations. Liehr et al. studied the mass spectrum of benzyl alcohol after chemical ionization with isobutane and an electrostatic complex between  $BzOH_2^+$  and

isobutene was discussed for the  $[M + C_4H_9]^+$  species.<sup>[54]</sup> Studies of protonated ethyl cyanide and ethyl isocyanide by Bouchoux et al. also provided evidence for electrostatic complexes.<sup>[55]</sup> Protonated ethyl cyanide can be thought of as the adduct of HCN or HNC with ethyl cation. Both ions  $[EtCNH]^+$  and  $[EtNCH]^+$  isomerize by  $\beta$  elimination into weakly bound  $\pi$  complexes of ethene and  $[HCNH]^+$ . In these cation–olefin complexes, the interaction of the acidic hydrogen with the olefin is principally an electrostatic charge-induced dipole interaction.

All of the electrostatically bound cation–neutral complexes characterized to date contain cations with high-lying  $\sigma^*$  LUMOs. Most frequently the cation involved is a monoatomic cation (e.g.,  $Li^+$ ) but molecular cations also form electrostatic complexes. In contrast, no electrostatically bound cation–neutral complexes have been detected or postulated that would involve cations with valence electron sextets where the LUMO is part of the valence shell and low-lying. Such cations are intrinsically good acceptors and they always have been found to form covalently bound complexes of the type  ${}_{CS}D \rightarrow {}_{OS}A$ : methyl cation and water form protonated methanol, methyl cation and carbon monoxide form an acylium ion, methyl cation and dinitrogen form methyldiazonium ion, and so on. The approach of a donor to a cation with a valence electron sextet, in the absence of isomerization of the type discussed, is usually characterized by a single-well potential energy diagram with the minimum representing the covalently bound complex as the sole minimum (A in Scheme 4).<sup>[56]</sup> Ab initio calculations at correlated levels



Scheme 4. Possible potential energy surface characteristics for the approach of a donor molecule to a cation.

suggest that the approach of  $N_2$  to nonclassical ethyl cation involves a local minimum that corresponds to an electrostatic complex (B).<sup>[57]</sup> In other words, the covalently bound complex  ${}_{CS}D \rightarrow {}_{OS}A$  and an electrostatically bound complex  ${}_{CS}D \cdots {}_{OS}A$  both exist on the potential energy surface. The activation barrier between the minima might be due to the transition from nonclassical to classical ethyl cation in the window of the  $N_2$  approach. Petrie and Bohme recently presented circumstantial evidence for such a double-well potential energy diagram for the approach of  $NH_3$  to fullerene cation.<sup>[58]</sup> Even if such a local minimum  ${}_{CS}D \cdots {}_{OS}A$  existed, the potential energy well for the electrostatically bound complex is rather shallow and it is much higher in energy than the covalently bound system  ${}_{CS}D \rightarrow {}_{OS}A$ . It would appear reasonable to assume this to be the general case. However, the potential energy surface characteristics of “benzylidiazonium ion” presented here exemplify the unprecedented scenario C where the interaction between a polarizable neutral molecule and a cation with a valence LUMO results in the preferential formation of an electrostatic complex and not the formation of a covalently bound complex. The ab initio calculations show that the interaction of  $N_2$  with benzyl cation **1** results

in an electrostatically bound complex as the most stable structure. A covalently bound benzyldiazonium ion **2** does exist as a stationary structure on the potential energy surface but it is much higher in energy and is a transition-state structure for automerization of the electrostatic complex.

The inability of  $N_2$  to engage in dative bonding with **M-1** shows that the LUMO is high in energy and not localized at the exocyclic carbon center (Figure 2). Charge delocalization in **M-1** is highly effective; this is reflected in the high barrier to  $CH_2$  rotation and the shortening of the  $C_{ipso}-CH_2$  bond in **M-1** as compared to **TS-1**. Only when the  $\pi$  interaction of the phenyl group with the  $CH_2$  group is interrupted and replaced by only a minor hyperconjugative interaction does the LUMO become localized at the  $CH_2$  carbon and available for dative bonding. But even then the Lewis acidity of **TS-1** remains low and the cross-section **2a** (Figure 4) shallow: the methyl cation affinity<sup>[5, 11]</sup> of  $N_2$  is  $44.0 \text{ kcal mol}^{-1}$  and a magnitude higher than the binding energy of  $N_2$  in **2A**. Aside from being an excellent  $\pi$  donor in conformation **2c**, the phenyl group also is a very effective  $\sigma$  donor and capable of delocalizing positive charge even in the conformation **2a**.

Molecular orbital theory is a useful aid for the rationalization of structural and energetic data. One should keep in mind, however, that only the total electron density is physically observable and that FMO theory merely represents an approximation to the true electron density deformations associated with chemical interaction. In Figure 5, we present graphical representations of the gradient vector fields of the total electron density distributions computed at the MP2(full)/6-31 G\* level for **1** and **2**. The color coding reflects the magnitude of the electron density and was selected such that the red regions describe the shape of the molecule ( $\rho > 0.01 \text{ e a}_0^{-3}$ );  $\pi$  bonding is indicated by blue coloring in the bonding region. The efficient  $\pi$ -dative bonding across the  $C_{ipso}-CH_2$  bond in **M-1** is clearly shown by comparison of the gradient vector fields of **M-1** and **TS-1** in the  $\pi$  planes (Figure 5, top center and top right). Rotation about the  $C_{ipso}-CH_2$  bond leads to a narrowing of the  $\pi$  region and a general decrease of the magnitude of the density in the  $C_{ipso}-CH_2$  region. The gradient vector field lines in **M-1** are indicative of strong  $\pi$  bonding as the GVF lines in bonding region are almost parallel to the zero-flux surface over a wide area. As can be seen, both of these features are absent in **TS-1** and the  $N_2$  systems **2A** and **2C'**, while they are clearly maintained in the electrostatic complex **2C**. The  $Ph \rightarrow CH_2$   $\pi$ -dative bond is broken only when a closer  $N_2$  approach to the methylene group is forced, as in model **2C'**, or is made impossible by conformation, as in the transition-state structure **2A**. The gradient vector fields of **2C** and **2A** show the drastic differences in the C–N bonding situations. While a “C–N bond” is formed in **2A** (density increase in C–N bonding region, anisotropic density deformation), the outer regions of the electron density of **1** and  $N_2$  barely touch in **2C**. **2A** and **2C** are a very good demonstration of the fact that electron density deformations in the “bonding region” and bond dissociation energies are not related in the simple fashion that is often assumed. This case illustrates better than any other that the binding energy is the result of energy changes that are not limited to the “bonding region” in the molecule. Characterization of the electron density distribution in the “bonding region” cannot describe bond strength.<sup>[5a, 59]</sup>

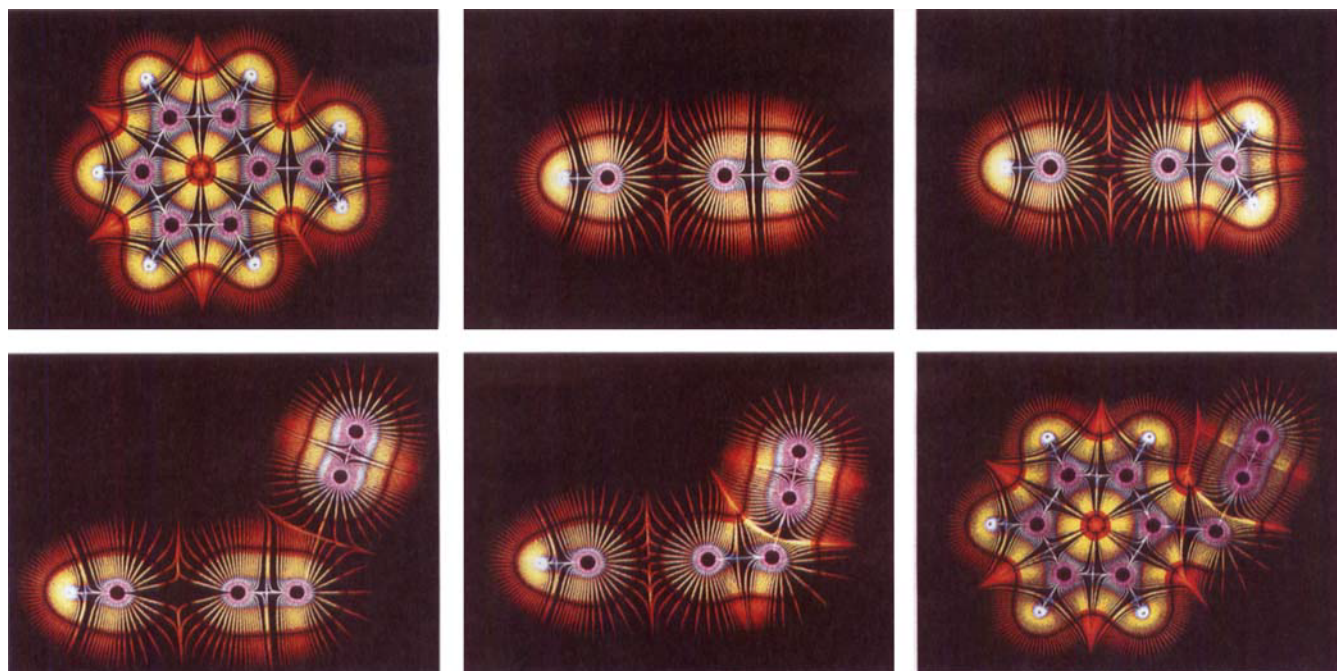


Figure 5. Graphical representations of the electron-density color-coded gradient vector fields of the electron density distributions of the benzyl cations **M-1** (top left and center) and **TS-1** (top right) and of the electrostatic complex **2C** (bottom, left), of the model structure **2C'** (bottom, center), and of the benzylidiazonium ion transition-state structure **2A** (bottom, right). The color coding reflects the magnitude of the electron density (pink 3–0.7, blue 0.35–0.3, yellow 0.2–0.1, red 0.05–0.01  $e a_0^{-3}$ ). The bond paths and the cross-sections of the zero-flux surfaces also are shown; the bond critical points occur at their intersections.

**Dinitrogen catalysis of cation rotational automerization:** Bohme et al. recently described the  $N_2$ -catalyzed isomerization of  $CH_3-NO_2^+$  to  $CH_3-ONO^+$ .<sup>[60]</sup> The catalytic action was attributed to the stabilization of  $CH_3^+$  in the aggregate  $O_2N \cdots CH_3-N_2^+$  during  $NO_2$  rotation and reconnection. By analogy, the potential energy characteristics of “benzylidiazonium ion” are best described as an  $N_2$ -catalyzed *rotational* isomerization of the benzyl cation. The rotational barrier of  $E_A(\mathbf{1}) = 47.7 \text{ kcal mol}^{-1}$  is drastically reduced to  $E_A(\mathbf{2}) = 27.8 \text{ kcal mol}^{-1}$  by  $N_2$  complexation. For the rotational isomerization to progress, the  $\pi$ -dative bond from the phenyl ring to the  $CH_2$  groups needs to be broken; the incipient “localized” carbenium ion is stabilized by  $N_2$ . Dative  $\sigma$ -bond formation between the  $CH_2$  carbon of benzyl cation and  $N_2$  is not competitive with dative  $\pi$ -bond formation between the  $CH_2$  group and the phenyl  $\pi$  system. Only when the benzyl cation undergoes an automerization by  $CH_2$  rotation does a closer approach of  $N_2$  become energetically beneficial. One closely related cation–donor system is protonated ethyl nitrate. Aschi et al. very recently reported that the isomers  $EtOH \cdots NO_2^+$  and  $[EtONO_2H]^+$  are almost isoenergetic, and MP2/6-31 G\* computations showed the  $EtOH \cdots NO_2^+$  isomer to be an electrostatic complex with a long O–N bond of  $> 2.3 \text{ \AA}$ .<sup>[61]</sup> Again, the dative O  $\rightarrow$  N bond formation is not competitive with the intramolecular stabilization of  $NO_2$  by  $\pi$  bonding.

## Conclusion

The potential energy surface characteristics of “benzylidiazonium ion” show for the first time that the interaction of a donor with a cation that has a valence electron sextet, and hence a

valence LUMO, may lead to the preferential formation of an electrostatic complex as opposed to the formation of the commonly encountered dative or covalently bound complex. The electrostatic complex is energetically preferred because dative  $\sigma$ -bond formation between the  $CH_2$  carbon of the benzyl cation and  $N_2$  is not competitive with dative Ph  $\rightarrow$   $CH_2$   $\pi$ -bond formation. This result suggests that, in general, electrostatic cation–molecule complexes involving a cation with an unfilled valence shell have to be expected whenever intramolecular stabilization mechanisms are more efficient than the formation of a dative or covalent bond to the cation center. Hence, the binding energy between the unsubstituted parent cation (here methyl cation) and the neutral donor provides a good estimate for the lower limit of the magnitude of the intramolecular stabilization necessary to prevent dative bond formation in the substituted cation. For example, the binding energy of methylidiazonium ion is  $44 \text{ kcal mol}^{-1}$ , and the electrostatic complex **2C** exists because the intramolecular stabilization of the  $-CH_2$  center in benzyl cation by the phenyl group ( $> 47 \text{ kcal mol}^{-1}$  as measured by the rotational barrier) exceeds the methyl cation affinity of  $N_2$ . Aside from the systems  $[H_{3-n}R_nX]^m+ \cdots$  donor with X = C,  $n = 3, m = 1$ , donor =  $N_2$ , these considerations of course apply generally to all kinds of systems in which any of these variables, or any combination of them, is altered. Variations of the identity of the atom X of the acceptor, of the charge of the acceptor, of the type and number of stabilizing groups attached, and of the nature of the donor molecule present opportunities in the search for the preferential formation of other such electrostatic complexes. For example, multiply donor-substituted carbenium ions clearly make promising candidates. Complexes between neutral acceptors, possibly with several stabilizing groups attached, and with neutral donors (e.g.,  $N_2$  complexes of donor-



substituted boranes, germanes and so on) are the most likely candidates for purely electrostatic complexes; some of these neutral systems are known.<sup>[16b, 49]</sup> With regard to the specific system considered here, the results presented provide evidence in support of White's inert-molecule-separated ion pair hypothesis<sup>[20]</sup> in that they show that C–N cleavage of an incipient benzyldiazonium ion occurs in the gas phase and is likely to be facile in general. It will be interesting to explore in future how the presence of a counterion affects the nature of the benzyl cation–dinitrogen interaction. It will also be of interest to investigate the effects exerted by substituents attached to the phenyl ring on the nature of the “benzyldiazonium ion”. In the light of the shallow nature of the energy minimum of electrostatic complexes, small structural and electronic changes may well have significant geometric consequences that may be reflected in product distributions.

**Acknowledgment:** We thank Dr. James Fishbein for valuable discussions. This research was conducted using the resources of the Cornell Theory Center, which receives major funding from the National Science Foundation and New York State, with additional support from the Advanced Research Projects Agency, the National Center for Research Resources at the National Institutes of Health, IBM Corporation, and the members of the Corporate Research Institute.

Received: January 8, 1997 [F 571]

- [1] For comprehensive reviews, see: H. Zollinger, *Diazo Chemistry I and Diazo Chemistry II*, VCH, Weinheim (Germany), **1994** and **1995**, respectively.
- [2] W. Ljijnski, *Chemical Structure of Nitrosamines Related to Carcinogenesis, in Nitrosamines and Related N-Nitroso Compounds* (Eds.: R. N. Loepky, C. J. Michejda), *ACS Symp. Ser.* **1994**, 553. American Chemical Society, Washington (DC), p. 251.
- [3] D. Brosch, W. Kirmse, *J. Org. Chem.* **1993**, 58, 1118, and references cited therein.
- [4] a) J. Hovinen, J. Fishbein, *J. Am. Chem. Soc.* **1992**, 114, 366; b) J. Hovinen, J. I. Finneman, S. N. Satapathy, J. Ho, J. C. Fishbein, *ibid.* **1992**, 114, 10321; c) J. I. Finneman, J. Ho, J. C. Fishbein, *ibid.* **1993**, 115, 3016; d) J. Ho, J. C. Fishbein, *ibid.* **1994**, 116, 6611.
- [5] a) R. Glaser, G. S.-C. Choy, M. K. Hall, *J. Am. Chem. Soc.* **1991**, 113, 1109; b) C. J. Horan, R. Glaser, *J. Phys. Chem.* **1994**, 98, 3989; c) R. Glaser, G. S.-C. Choy, *J. Am. Chem. Soc.* **1993**, 115, 2340; d) R. Glaser, G. S.-C. Choy, *J. Phys. Chem.* **1991**, 95, 7682.
- [6] Reviews on dative bonding theory: a) A. Haaland, *Angew. Chem. Int. Ed. Engl.* **1989**, 28, 992, and references cited therein; b) K. R. Leopold, M. Canagaratna, J. A. Phillips, *Acc. Chem. Res.* **1997**, 30, 57, and references cited therein.
- [7] a) R. Glaser, C. J. Horan, P. E. Haney, *J. Phys. Chem.* **1993**, 97, 1835; b) R. Glaser, C. J. Horan, G. S.-C. Choy, B. L. Harris, *ibid.* **1992**, 96, 3689; c) R. Glaser, *J. Comput. Chem.* **1990**, 11, 663; d) R. Glaser, *J. Phys. Chem.* **1989**, 93, 7993.
- [8] a) R. Glaser, C. J. Horan, *J. Org. Chem.* **1995**, 60, 7518; b) M. A. Vincent, L. Radom, *J. Am. Chem. Soc.* **1978**, 100, 3306.
- [9] a) G. S. Chen, R. Glaser, C. L. Barnes, *J. Chem. Soc. Chem. Commun.* **1993**, 1530; b) R. Glaser, G. S. Chen, C. L. Barnes, *Angew. Chem. Int. Ed. Engl.* **1992**, 31, 740.
- [10] a) R. Glaser, C. J. Horan, *Can. J. Chem.* **1996**, 74, 1200; b) R. Glaser, C. J. Horan, E. Nelson, M. K. Hall, *J. Org. Chem.* **1992**, 57, 215.
- [11] a) M. S. Foster, J. L. Beauchamp, *J. Am. Chem. Soc.* **1972**, 94, 2425; b) M. S. Foster, A. D. Williamson, J. L. Beauchamp, *Int. J. Mass. Spectrom. Ion Phys.* **1974**, 15, 429; c) T. B. McMahon, T. Heinis, G. Nicol, J. K. Hovey, P. Kebarle, *J. Am. Chem. Soc.* **1988**, 110, 7591; d) M. N. Glukhovisev, J. E. Szulejko, T. B. McMahon, J. W. Gauld, A. P. Scott, B. J. Smith, A. Pross, L. Radom, *J. Phys. Chem.* **1994**, 98, 13099.
- [12] a) J. F. McGarrity, T. Smyth, *J. Am. Chem. Soc.* **1980**, 102, 7303; b) J. F. McGarrity, D. P. Cox, *ibid.* **1983**, 105, 3961; c) see also: J. P. Pezacki, B. D. Wagner, C. S. Q. Lew, J. Warkentin, J. Luszyk, *ibid.* **1997**, 119, 1789.
- [13] a) The stable so-called 1-(*para*-benzyldiazonium)diethylenetriamine pentaacetic acids (aDTPA) used in antibody labeling and tumor-imaging studies (ref. [13b]) are not actually benzyldiazonium ions but *para*-diazonio toluenes (refs. [13c and d]); b) M. Maeda, M. Shoji, T. Kawagoshi, R. Futatsuya, T. Honda, L. Brady, *W. Cancer (Philadelphia)* **1994**, 73, 800; c) M. W. Brechbiel, O. A. Gansow, R. W. Atcher, J. Schlom, J. Esteban, D. E. Simpson, D. Colcher, *Inorg. Chem.* **1986**, 25, 2772; d) M. W. Sundberg, C. F. Meares, D. A. Goodwin, C. I. Diamanti, *J. Med. Chem.* **1974**, 17, 1304.
- [14] L. Capuano, H. Dürr, R. Zander, *Liebigs Ann. Chem.* **1969**, 721, 75.
- [15] Studies of *para*-nitrophenyldiazomethane and of a series of its diazo-C substituted derivatives: W. Jugelt, L. Berseck, *Tetrahedron* **1970**, 5581.
- [16] a) H. Dahn, G. Diderich, *Helv. Chim. Acta* **1971**, 54, 1950; b) G. Diderich, H. Dahn, *ibid.* **1972**, 55, 1.
- [17] J. I. Finneman, J. C. Fishbein, *J. Am. Chem. Soc.* **1994**, 59, 6251.
- [18] a) J. I. Finneman, J. C. Fishbein, *J. Am. Chem. Soc.* **1995**, 117, 4228; b) J. I. Finneman, J. C. Fishbein, *ibid.* **1996**, 118, 7134.
- [19] a) C. C. Jones, M. A. Kelly, M. L. Sinnott, P. J. Smith, *J. Chem. Soc. Chem. Commun.* **1980**, 322; b) C. C. Jones, M. A. Kelly, M. L. Sinnott, P. J. Smith, G. T. Tzozos, *J. Chem. Soc. Perkin Trans. 2* **1982**, 1655, and references cited therein.
- [20] E. H. White, K. W. Field, W. H. Hendrickson, P. Dzadzic, D. F. Roswell, S. Paik, P. W. Mullen, *J. Am. Chem. Soc.* **1992**, 114, 8023, and references cited therein.
- [21] W. J. Hehre, L. Radom, P. v. R. Schleyer, J. A. Pople, *Ab Initio Molecular Orbital Theory*, Wiley, New York, **1986**.
- [22] a) M. J. Frisch, M. Head-Gordon, J. A. Pople, *Chem. Phys. Lett.* **1990**, 166, 275; b) M. Head-Gordon, T. Head-Gordon, *ibid.* **1994**, 220, 122.
- [23] R. Krishnan, J. A. Pople, *Int. J. Quant. Chem.* **1978**, 14, 91.
- [24] a) QCI: J. A. Pople, M. Head-Gordon, K. Raghavachari, *J. Chem. Phys.* **1987**, 87, 5968; b) CC: R. J. Bartlett, G. D. Purvis, *Int. J. Quant. Chem.* **1978**, 14, 516; c) for a recent comparison, see: Z. He, E. Kraka, D. Cremer, *ibid.* **1996**, 57, 157.
- [25] a) J. A. Pople, A. P. Scott, M. W. Wong, L. Radom, *Isr. J. Chem.* **1993**, 33, 345; b) the scaling factors differ from the ones determined for small diazonium ions in ref. [7a] and they were used since most of the VZPE resides in modes of the hydrocarbon fragment.
- [26] *Gaussian94*, Revision C.3: M. J. Frisch, G. W. Trucks, H. B. Schlegel, P. M. W. Gill, B. G. Johnson, M. A. Robb, J. R. Cheeseman, T. Keith, G. A. Petersson, J. A. Montgomery, K. Raghavachari, M. A. Al-Laham, V. G. Zakrzewski, J. V. Ortiz, J. B. Foresman, J. Cioslowski, B. B. Stefanov, A. Nanayakkara, M. Challacombe, C. Y. Peng, P. Y. Ayala, W. Chen, M. W. Wong, J. L. Andres, E. S. Replogle, R. Gomperts, R. L. Martin, D. J. Fox, J. S. Binkley, D. J. Defrees, J. Baker, J. J. P. Stewart, M. Head-Gordon, C. Gonzalez, J. A. Pople, Gaussian, Pittsburgh (PA), **1995**.
- [27] Spartan, by Wavefunction, Irvine (CA).
- [28] “CCGVF: Color-Coded Gradient Vector Fields”, R. Glaser, D. Farmer, University of Missouri–Columbia, **1995**, unpublished results.
- [29] R. F. W. Bader, *Atoms in Molecules, A Quantum Theory*, Oxford University Press, New York, **1990**.
- [30] J.-L. Abboud, W. J. Hehre, R. W. Taft, *J. Am. Chem. Soc.* **1976**, 98, 6072.
- [31] The thermodynamics of **1** is now well established: a) T. Baer, J. C. Morrow, J. D. Shao, S. Olesik, *J. Am. Chem. Soc.* **1988**, 110, 5633; b) G. C. Eiden, J. C. Weisshaar, *J. Chem. Phys.* **1991**, 95, 6194.
- [32] For a recent FT mass spectrometric study of benzyl cation vs. tropylium ion populations, see: M. Bensimon, G. Zhao, T. Gäumann, *Spectros. Int. J.* **1989**, 7, 193, and references cited therein.
- [33] J. C. Traeger, B. M. Kompe, *Int. J. of Mass Spectrom. Ion Processes* **1990**, 101, 111.
- [34] a) A. E. Dorigo, Y. Li, K. N. Houk, *J. Am. Chem. Soc.* **1989**, 111, 6942; b) see also ref. [41c].
- [35] T. Ohwada, K. Shudo, *J. Am. Chem. Soc.* **1989**, 111, 34.
- [36] K. Nakata, M. Fujio, Y. Saeki, M. Mishima, Y. Tsuno, K. Nishimoto, *J. Phys. Org. Chem.* **1996**, 9, 561.
- [37] a) G. C. Eiden, K.-T. Lu, J. Badenhop, F. Weinhold, J. C. Weisshaar, *J. Chem. Phys.* **1996**, 104, 8886; b) G. C. Eiden, F. Weinhold, J. C. Weisshaar, *ibid.* **1991**, 95, 8665.
- [38] Note that Traeger and Kompe (ref. [33]) did examine the relative stabilities of benzyl and tropylium ions at the MP2 level but those calculations employed a small unpolarized basis set and they were based on RHF/3-21G structures.
- [39] a) Dideuteroethylene: J. E. Douglas, B. S. Rabinovitch, F. S. Looney, *J. Chem. Phys.* **1955**, 23, 315; b) butene-2: B. S. Rabinovitch, K. W. Michel, *J. Am. Chem. Soc.* **1959**, 81, 5065; c) L. Giroux, M. H. Back, R. A. Back, *Chem. Phys. Lett.* **1989**, 154, 610.
- [40] M. Mishima, K. Arima, S. Usui, M. Fujio, Y. Tsuno, *Chem. Lett.* **1987**, 1047.
- [41] a) C. Hansch, A. Leo, R. W. Taft, *Chem. Rev.* **1991**, 91, 165, and references cited therein; b) T. L. Amyes, J. P. Richard, *J. Am. Chem. Soc.* **1990**, 112, 9507, and references cited therein; c) T. L. Amyes, J. P. Richard, M. Novak, *ibid.* **1992**, 114, 8032.
- [42] P. Wan, B. Chak, *J. Chem. Soc. Perkin Trans. 2* **1986**, 1751.
- [43] M. D. Heagy, G. A. Olah, G. K. S. Prakash, J. S. Lomas, *J. Org. Chem.* **1995**, 60, 7355.
- [44] E. T. M. Selim, M. A. Rabbih, M. A. Fahmey, M. F. Hawash, *Int. J. Mass Spectrom. Ion Processes* **1994**, 134, 119.
- [45] Electron correlation effects are known to reduce the dissociation energies of stable diazonium ions, and we note that just the opposite is true for the “unstable” diazonium ions **2A** and **2C**.
- [46] a) U. Olsher, R. M. Izatt, J. S. Bradshaw, N. K. Dalley, *Chem. Rev.* **1991**, 91, 137, and references cited therein; b) K<sup>+</sup> and benzene: J. Sunner, K. Nishizawa,

- P. Kebarle, *J. Phys. Chem.* **1981**, *85*, 1814; c) K<sup>+</sup> and DMSO, DMA, DMF, and acetone: J. Sunner, P. Kebarle, *J. Am. Chem. Soc.* **1984**, *106*, 6135.
- [47] S. Ikuta, *Chem. Phys.* **1985**, *95*, 235.
- [48] It is not the purpose of this paper to distinguish between dative and covalent bonding. The term "covalently bound" is used for complexes with short distances between the electron-deficient center of the cation and the donor atom of the neutral organic irrespective of whether this interaction involves dative or covalent bonding. Our focus lies on the distinction of these complexes from purely electrostatically bound complexes.
- [49] K. C. Janada, L. S. Bernstein, J. M. Steed, S. E. Novick, W. Klemperer, *J. Am. Chem. Soc.* **1978**, *100*, 8074.
- [50] S. G. Lias, *J. Phys. Chem.* **1984**, *88*, 4401.
- [51] For isomerizations involving CH<sub>3</sub><sup>+</sup> transfer, see for example: a) D. K. Sen Sharma, P. Kebarle, *J. Am. Chem. Soc.* **1982**, *104*, 19; b) M. Speranza, G. Laguzzi, *ibid.* **1988**, *110*, 30; c) M. Attina, F. Cacace, A. Ricci, *Angew. Chem. Int. Ed. Engl.* **1991**, *30*, 1457.
- [52] a) Review: C. R. Moylan, J. I. Brauman, *The Double-Well Model for Ion-Molecule Reactions*, in *Advances in Classical Trajectory Methods*, Vol. 2, JAI, **1994**, p. 95–114; b) J. L. Wilbur, J. I. Brauman, *J. Am. Chem. Soc.* **1994**, *116*, 5839, 9216, and references cited therein.
- [53] K. Norrman, T. B. McMahon, *J. Am. Chem. Soc.* **1996**, *118*, 2449.
- [54] J. G. Liehr, G. A. Brenton, J. H. Beynon, J. A. McCloskey, W. Blum, W. J. Richter, *Helv. Chim. Acta* **1981**, *64*, 835.
- [55] G. Bouchoux, M. T. Nguyen, P. Longevialle, *J. Am. Chem. Soc.* **1992**, *114*, 10000.
- [56] The same is also true for the approach of a donor molecule to a radical cation. Electrostatic complexes may occur as local minima, but these complexes undergo covalent bond formation leading to a distonic cation. For a good example, see: G. Bouchoux, Y. Hoppilliard, J. Tortajada, *Int. J. Mass Spectrom. Ion Processes* **1989**, *90*, 197.
- [57] R. Glaser, unpublished results.
- [58] S. Petrie, D. K. Bohme, *Can. J. Chem.* **1994**, *72*, 577.
- [59] N. D. Epiotis, *Deciphering the Chemical Code – Bonding Across the Periodic Table*, VCH, Weinheim (Germany), **1996**, p. 137.
- [60] V. Baranov, S. Petrie, D. K. Bohme, *J. Am. Chem. Soc.* **1996**, *118*, 4500.
- [61] M. Aschi, F. Cacace, G. d. Petris, F. Pepl, *J. Phys. Chem.* **1996**, *100*, 16522.